PROCEEDINGS OF SCIENCE

Non-factorisable contributions to t-channel single top and VBF Higgs production

Konstantin Asteriadis,[a,b] **Christian Brønnum-Hansen,**[c,*] **Jérémie Juvin-Quarroz,**[c] **Chiara Signorile-Signorile**[c,d] **and Chen-Yu Wang**[c,d]

[a] *High Energy Theory Group, Physics Department, Brookhaven National Laboratory, Upton, NY 11973, USA*

[b] *Institut für Theoretische Physik, Universität Regensburg, 93040 Regensburg, Germany*

[c] *Institute for Theoretical Particle Physics, KIT, 76131 Karlsruhe, Germany*

[d] *Max-Planck-Institut für Physik, Boltzmannstrasse 8, 85748 Garching, Germany*

E-mail: christian.broennum-hansen@partner.kit.edu

We discuss non-factorisable contributions to two processes, t-channel single top production and Higgs production in vector boson fusion. Non-factorisable contributions are often neglected since they enter for the first time at next-to-next-leading order in perturbative calculations in the strong coupling constant and are colour-suppressed. However, due to a peculiar enhancement in the double-virtual contribution, these corrections can reach percent level in kinematic distributions, thus making them comparable in magnitude to predictions in the factorisable approximation. We present phenomenological results for both processes in proton-proton collisions at 13 TeV.

TTP23-058, P3H-23-097

16th International Symposium on Radiative Corrections: Applications of Quantum Field Theory to Phenomenology (RADCOR2023)
28th May - 2nd June, 2023
Crieff, Scotland, UK

*Speaker

PoS(RADCOR2023)011

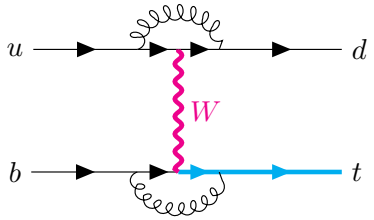

(a) Factorisable diagram contributing to the double-virtual amplitude.

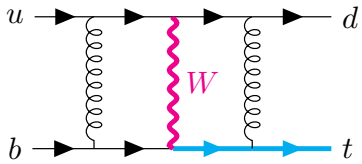

(b) Non-factorisable diagram contributing to the double-virtual amplitude.

Figure 1: Examples of two-loop Feynman diagrams contributing to t-channel single top production at NNLO in the strong coupling constant.

1. Introduction

About a fifth of top quarks produced at the Large Hadron Collider (LHC) come from the t-channel single top production mechanism, $q + b \to q' + t$, where two incoming quarks exchange a (colourless) weak boson. In addition to measurements of the top quark mass and width, this process can be used to probe the CKM matrix element V_{tb} directly and to constrain the bottom quark parton distribution function (PDF).

In the factorisation approximation, where gluon exchanges between the two incoming quark lines are neglected (see Fig. 1 for diagram examples of the factorisable and non-factorisable kind), theoretical predictions for t-channel single top production are known to next-to-next-to-leading order (NNLO) in the strong coupling constant [1–4]. These corrections affect the total cross section at the level of a few percent with respect to NLO. Given such high theoretical accuracy, it is interesting to explore the impact of the non-factorisable contributions as well. The non-factorisable contributions are colour-suppressed by a factor of $N_C^2 - 1 = 8$, but could receive an enhancement due to a peculiar virtual effect attributed to remnants of the Glauber phase.

Vector boson fusion (VBF), $q + Q \to q' + Q' + H$, has the second-largest cross section for Higgs production at the LHC. This production mechanism is particularly interesting for Higgs searches due to its clear kinematic signature. Its direct sensitivity to the couplings between the Higgs boson and W and Z bosons allows for a detailed exploration of their strengths and Lorentz structures.

Similarly to single top production, Higgs production in VBF also involves a t-channel exchange of weak bosons. Relying on the same arguments discussed in the case of single top production, based on colour suppression, the fixed-order predictions for this process also admits a factorisation approximation. For this approximation, predictions are known differentially to NNLO in the strong coupling constant [7–10] and inclusively even to N^{3}LO [11]. The latter is a correction at the permille level and smaller than the double-virtual, non-factorisable contribution which was calculated in the eikonal approximation in Ref. [12].

In these proceedings, we present the results of a full calculation of the non-factorisable contribution to t-channel single top production based on the original works in Refs. [5, 6]. In addition, we present phenomenological results for VBF Higgs production by combining the non-factorisable double-virtual calculation [12] with the double-real and real-virtual contributions as presented in Ref. [13].

2. Calculation

For both processes, $q+b \to q'+t$ and $q+Q \to q'+Q'+H$, we are faced with an NNLO QCD computation requiring the construction of an infrared-finite cross section which can be integrated over fiducial phase space in four dimensions. In order to obtain fully differential predictions, we treat infrared divergences arising from double-virtual, real-virtual and double-real corrections by means of a variant of the nested soft-collinear subtraction scheme [14]. The subtraction procedure for non-factorisable corrections at NNLO is remarkably simple due to the absence of non-Abelian diagrams as well as the absence of collinear singularities. The application of this scheme to the non-factorisable cases considered here was discussed in detail in Refs. [6, 13].

Once the substraction procedure is established, the necessary amplitudes must be supplied. The double-virtual correction requires the calculation of two-loop scattering amplitudes. An example Feynman diagram contributing to the non-factorisable two-loop amplitude for single top production is shown on the right in Fig. 1. The details of this calculation is given in Ref. [5] and only briefly commented here. While the integral reduction procedure through integration-by-parts identities is managable with modest computational expense using publically available software, analytic expressions for the full set of 428 master integrals are not available. The numerical method of auxiliary mass flow [15] is a computationally efficient alternative and since there are only two kinematic invariants, it is possible to perform a scan of the phase space. We estimate the double-virtual contribution by sampling over 100k phase space points.

The situation is however different for VBF Higgs production. With five kinematic invariants as well as internal masses, the integral reduction is prohibitively complex and the phase space dimension too high for a numerical scan. However, the calculation is greatly simplified by employing the eikonal approximation, which is justified by the typical forward kinematics of this process [12]. This approximation simplifies the involved Feynman integrals by separating the kinematics along and transverse to the beamline, which makes an analytic calculation tractable.

For the real-virtual computation we need one-loop amplitudes with up to one additional gluon in the final state. The details of the single top production calculation and the necessary measures to achieve numerical stability are discussed in Ref. [6]. For VBF Higgs production, computer code for evaluating the one-loop matrix elements for $q+Q \to q'+Q'+H$ and $q+Q \to q'+Q'+H+g$ was kindly provided by the authors of Ref. [16]. With some minor changes, this code provided us with the non-factorisable contribution of the real-virtual correction. However, it was non-trivial to achieve sufficient numerical stability around singular limits. This is discussed in more detail in Ref. [13].

3. Results

We consider proton-proton collisions at 13 TeV, but otherwise use slightly different setups for the two processes to ease comparison with existing literature. In both setups the CKM matrix is taken to be a unit matrix.

For single top production we obtain the leading-order (LO) cross section and kinematic distributions using the leading-order PDFs `CT14_lo`, but use the `CT14_nnlo` PDF set for the NNLO factorisable contribution. The strong coupling constant is provided by the `CT14_nnlo` PDF set

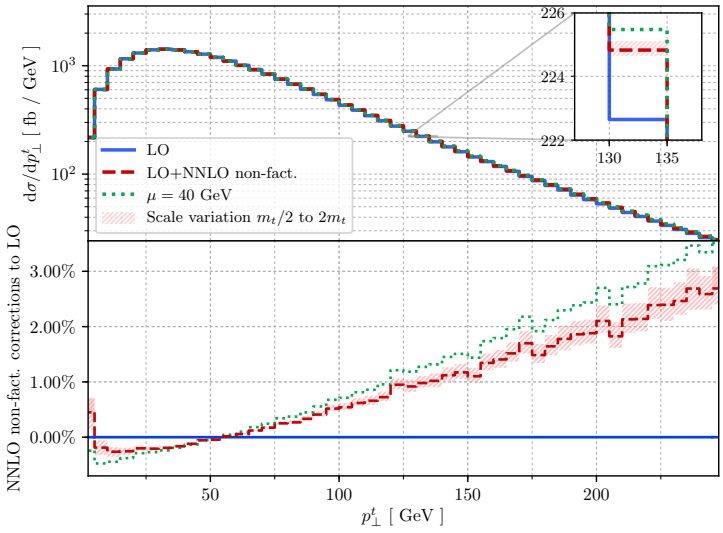

Figure 2: Top quark transverse momentum distribution. The leading-order distribution is marked with a blue, solid line, while the red, dashed line corresponds to non-factorisable contributions through NNLO at $\mu = m_t$. The scale is variated between $\mu = m_t/2$ and $\mu = 2m_t$. The green, dotted line corresponds to the scale $\mu = 40$ GeV. The lower pane shows the ratio of non-factorisable corrections to the leading-order distribution. Figure from Ref. [6]

.

and it evaluates to $\alpha_s(M_Z) = 0.118$. We set the vacuum expectation value of the Higgs field, $v = 246.2$ GeV, the mass of the W boson, $M_W = 80.379$ GeV, and the pole mass of the top quark, $m_t = 173.0$ GeV.

The non-factorisable NNLO QCD correction to the single top production cross section is

$$\frac{\sigma_{pp\to X+t}}{1\text{ pb}} = 117.96 + 0.26\left(\frac{\alpha_s(\mu_R)}{0.108}\right)^2, \tag{1}$$

where the first term on the right-hand side is the LO cross section. In the second term we have emphasised the freedom of choice of renormalisation scale in the non-factorisable contribution since it enters at NNLO for the very first time. For $\mu_R = \mu_F = m_t$ the impact of non-factorisable corrections to LO is about 0.2%. However, if a lower scale is chosen, such as $\mu_R = 40$ GeV, which corresponds to the typical momentum transfer in the t-channel, the correction grows to 0.35%.

In Figure 2 we show the distribution of the top quark transverse momentum. The correction is small, but with a clear dependence on transverse momentum. The shape largely follows that shown in Ref. [5] where only the double-virtual correction was considered and is hence consistent with the expectation that non-factorisable contributions are dominated by virtual corrections. In comparison with factorisable contributions presented in Ref. [4], the non-factorisable are smaller. However, around the peak of the distribution the corrections are very comparable in size.

For VBF Higgs production we consider the Higgs boson to be stable with a mass of $m_H = 125$ GeV. Vector boson masses are set to $M_W = 80.398$ GeV and $M_Z = 91.1876$ GeV with widths $\Gamma_W = 2.105$ GeV and $\Gamma_Z = 2.4952$ GeV. The weak couplings are derived from the Fermi constant $G_F = 1.16639 \times 10^{-5}$ GeV^{-2}.

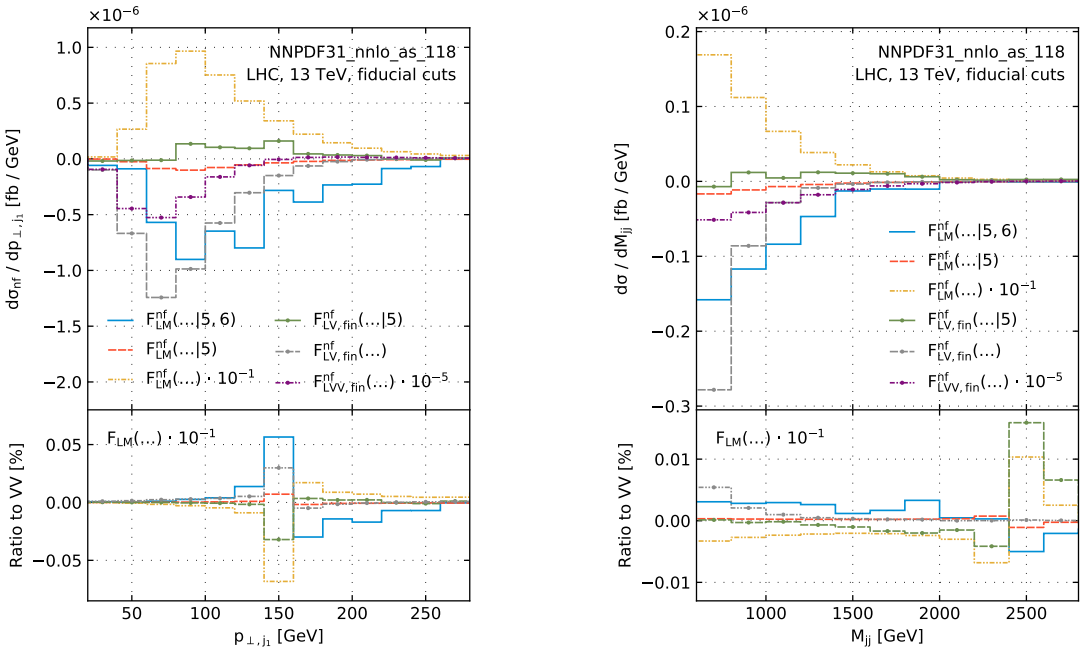

Figure 3: Non-factorisable contribution to the transverse momentum distributions of the leading jet (left) and to the distribution of the invariant mass of the tag-jet system (right). Separate contributions to the cross section are shown individually, full details are given in [13] where this figure is from. For each plot (and differently in upper and lower panes) contributions are scaled to be of similar orders. The lower pane shows the ratio with respect to double-virtual contributions.

We use the `NNPDF31-nnlo-as-118` PDFs with $\alpha_s(M_Z) = 0.118$. Here we employ the same dynamical scale for renormalisation and factorisation, $\mu_R = \mu_F = \mu$, with

$$\mu = \sqrt{\frac{m_H}{2}\sqrt{\frac{m_H^2}{4} + p_{\perp,H}^2}}\,. \tag{2}$$

We employ the inclusive anti-$k_\perp$ jet algorithm with $R = 0.4$. We require at least two jets with transverse momenta $p_{\perp,j} > 25$ GeV and rapidities $|y_j| < 4.5$. The two leading-$p_\perp$ jets must be well separated, $|y_{j_1} - y_{j_2}| > 4.5$ and with an invariant mass larger than 600 GeV. Finally, the two leading jets must be in separate hemispheres in the laboratory frame; this is enforced by requiring the product of their rapidities to be negative, $y_{j_1} y_{j_2} < 0$.

The non-factorisable NNLO QCD correction to the VBF cross section with cuts and dynamical scale choice applied as described above is found to be

$$\sigma_{\rm nf} = -3.1 \text{ fb}\,. \tag{3}$$

We note that $\sigma_{\rm nf}$ is a correction of around –0.4% of the fiducial cross section computed through NNLO QCD in the factorisation approximation [17] and is about a factor of ten smaller than the factorisable NNLO QCD corrections.

The fiducial cross section is completely dominated by the double-virtual contribution, which accounts for 99.99%. We only included the leading eikonal approximation for the double-virtual amplitude. However, as the sub-eikonal correction, which was recently calculated [18], reduces the double-virtual by $O(20\%)$, the strong dominance continues to hold. The dominance is also seen in all kinematic distributions considered. As demonstration we show the separate contributions to the transverse momentum distributions of the hardest jet and the distribution of the invariant mass of the pair of leading jets in Fig. 3.

In conclusion, we have completed the NNLO correction of both t-channel single top production and VBF Higgs production by calculating the non-factorisable contribution to the cross sections as well as the kinematic distributions. We find that the double-virtual contribution is dominant for both processes, but with sub-percent level corrections to the cross sections. In kinematic distributions however, the corrections can reach $O(1\%)$ and can in certain regions be comparable to the factorisable ones.

4. Acknowledgements

The authors thank Prof. Kirill Melnikov for contributing to the results quoted in this report. This research is partially supported by the Deutsche Forschungsgemeinschaft (DFG, German Research Foundation) under grant 396021762 - TTR 257. The research of K.A. is supported by the United States Department of Energy under Grant Contract DE-SC0012704. The work of C.B.H. presented here is supported by the Carlsberg Foundation, grant CF21-0486.

References

[1] M. Brucherseifer, F. Caola and K. Melnikov, Phys. Lett. B **736** (2014), 58-63 doi:10.1016/j.physletb.2014.06.075 [arXiv:1404.7116 [hep-ph]].

[2] E. L. Berger, J. Gao, C. P. Yuan and H. X. Zhu, Phys. Rev. D **94** (2016) no.7, 071501 doi:10.1103/PhysRevD.94.071501 [arXiv:1606.08463 [hep-ph]].

[3] E. L. Berger, J. Gao and H. X. Zhu, JHEP **11** (2017), 158 doi:10.1007/JHEP11(2017)158 [arXiv:1708.09405 [hep-ph]].

[4] J. Campbell, T. Neumann and Z. Sullivan, JHEP **02** (2021), 040 doi:10.1007/JHEP02(2021)040 [arXiv:2012.01574 [hep-ph]].

[5] C. Brønnum-Hansen, K. Melnikov, J. Quarroz and C. Y. Wang, JHEP **11** (2021), 130 doi:10.1007/JHEP11(2021)130 [arXiv:2108.09222 [hep-ph]].

[6] C. Brønnum-Hansen, K. Melnikov, J. Quarroz, C. Signorile-Signorile and C. Y. Wang, JHEP **06**, 061 (2022) doi:10.1007/JHEP06(2022)061 [arXiv:2204.05770 [hep-ph]].

[7] P. Bolzoni, F. Maltoni, S. O. Moch and M. Zaro, Phys. Rev. Lett. **105** (2010), 011801 doi:10.1103/PhysRevLett.105.011801 [arXiv:1003.4451 [hep-ph]].

[8] P. Bolzoni, F. Maltoni, S. O. Moch and M. Zaro, Phys. Rev. D **85** (2012), 035002 doi:10.1103/PhysRevD.85.035002 [arXiv:1109.3717 [hep-ph]].

[9] M. Cacciari, F. A. Dreyer, A. Karlberg, G. P. Salam and G. Zanderighi, Phys. Rev. Lett. **115** (2015) no.8, 082002 [erratum: Phys. Rev. Lett. **120** (2018) no.13, 139901] doi:10.1103/PhysRevLett.115.082002 [arXiv:1506.02660 [hep-ph]].

[10] J. Cruz-Martinez, T. Gehrmann, E. W. N. Glover and A. Huss, Phys. Lett. B **781** (2018), 672-677 doi:10.1016/j.physletb.2018.04.046 [arXiv:1802.02445 [hep-ph]].

[11] F. A. Dreyer and A. Karlberg, Phys. Rev. Lett. **117** (2016) no.7, 072001 doi:10.1103/PhysRevLett.117.072001 [arXiv:1606.00840 [hep-ph]].

[12] T. Liu, K. Melnikov and A. A. Penin, Phys. Rev. Lett. **123** (2019) no.12, 122002 doi:10.1103/PhysRevLett.123.122002 [arXiv:1906.10899 [hep-ph]].

[13] K. Asteriadis, C. Brønnum-Hansen and K. Melnikov, [arXiv:2305.08016 [hep-ph]].

[14] F. Caola, K. Melnikov and R. Röntsch, Eur. Phys. J. C **77** (2017) no.4, 248 doi:10.1140/epjc/s10052-017-4774-0 [arXiv:1702.01352 [hep-ph]].

[15] X. Liu, Y. Q. Ma and C. Y. Wang, Phys. Lett. B **779** (2018), 353-357 doi:10.1016/j.physletb.2018.02.026 [arXiv:1711.09572 [hep-ph]].

[16] F. Campanario, T. M. Figy, S. Plätzer and M. Sjödahl, Phys. Rev. Lett. **111** (2013) no.21, 211802 doi:10.1103/PhysRevLett.111.211802 [arXiv:1308.2932 [hep-ph]].

[17] K. Asteriadis, F. Caola, K. Melnikov and R. Röntsch, JHEP **02** (2022), 046 doi:10.1007/JHEP02(2022)046 [arXiv:2110.02818 [hep-ph]].

[18] M. M. Long, K. Melnikov and J. Quarroz, JHEP **07** (2023), 035 doi:10.1007/JHEP07(2023)035 [arXiv:2305.12937 [hep-ph]].